Letter

Two- and Three-Dimensional ^{13}C−^{17}O Heteronuclear Correlation NMR Spectroscopy for Studying Organic and Biological Solids

Ivan Hung, Zhehong Gan, and Gang Wu*

Read Online

ACCESS | Metrics & More | Article Recommendations

ABSTRACT: We report two- and three-dimensional (2D and 3D) ^{13}C−^{17}O heteronuclear correlation solid-state NMR experiments under magic-angle spinning (MAS) conditions. These experiments utilize the D-RINEPT (Dipolar-mediated Refocused Insensitive Nuclei Enhanced by Polarization Transfer) scheme with symmetry-based $SR4_1^2$ recoupling blocks for coherence transfer between ^{13}C and ^{17}O nuclei. First, a 2D ^{17}O → ^{13}C correlation experiment was performed for the [1-^{13}C,^{17}O]-Gly/Gly·HCl cocrystal and [U-^{13}C, 1-^{17}O]-α/β-D-glucose samples. Second, a 2D ^{17}O → ^{13}C MQ-D-RINEPT correlation experiment where the indirect dimension incorporates the multiple-quantum MAS (MQMAS) scheme was tested for obtaining isotropic ^{17}O resolution with [U-^{13}C, 1-^{17}O]-α/β-D-glucose. Third, a new 3D ^{17}O → ^{13}C → ^{13}C correlation experiment was demonstrated where ^{17}O → ^{13}C and ^{13}C → ^{13}C correlations are achieved by D-RINEPT and DARR (Dipolar Assisted Rotational Resonance) sequences, respectively (thus termed as a 3D D-RINEPT/DARR OCC experiment). This new 3D ^{17}O NMR experiment is implemented with the aim for site-resolved solid-state ^{17}O NMR studies.

3D ^{17}O/^{13}C NMR
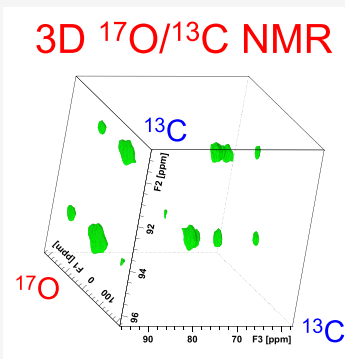
The oxygen element is an essential constituent of organic and biological molecules and its importance in the structure and function of these molecules can be readily appreciated. Unlike other key constituents of organic/biological molecules such as H, C, N, and P, the only NMR-active oxygen isotope, ^{17}O (I = 5/2, natural abundance 0.037%), has not been widely used in NMR spectroscopic studies of biological molecules.[1−6] Two major obstacles have contributed to the paucity of ^{17}O NMR studies of biological macromolecules such as proteins and nucleic acids. One is the difficulty of introducing ^{17}O-isotopes into biological molecules (i.e., ^{17}O-labeling) and the other is the intrinsically low spectral resolution often associated with a half-integer quadrupolar nucleus such as ^{17}O. In a recent study, Lin et al.[7] demonstrated that it is possible to incorporate [1-^{13}C,^{17}O]-doubly labeled amino acids into recombinant proteins so that selective protein backbone carbonyl groups are isotope labeled in the form of ^{13}C=^{17}O. Lin et al.[7] further proposed that this [1-^{13}C,^{17}O]-double labeling scheme can serve two purposes. First, it will be possible to use ^{13}C−^{17}O heteronuclear correlation spectroscopy to aid ^{17}O NMR signal assignment, because ^{13}C signal assignment can be readily achieved with the conventional solid-state ^{13}C and ^{15}N NMR approaches for uniformly ^{13}C/^{15}N labeled proteins. Second, it will also be possible to utilize the high spectral resolution in the ^{13}C dimension to separate overlapping ^{17}O NMR signals, which often suffer from second-order quadrupole broadenings even under magic-angle spinning (MAS) conditions. While two-dimensional (2D) heteronuclear correlation solid-state NMR spectroscopy

between quadrupolar and spin-1/2 nuclei has been widely reported in the literature,[8−12] the only attempt for ^{13}C−^{17}O correlation was the recent work by Keeler et al.,[13] where they successfully demonstrated the Z-Filtered Transferred-Echo Double Resonance (ZF-TEDOR) experiment on a sample of N-acetyl-[U-^{13}C,^{15}N; 70% ^{17}O]-L-Val-L-Leu. However, because the reported sensitivity of the ZF-TEDOR experiment was exceedingly low, it is necessary to develop new strategies that can improve both sensitivity and spectral resolution. We should also note that ^{13}C−^{17}O distance measurement[14−16] and observation of *J*-couplings between ^{13}C and ^{17}O nuclei[17,18] have been previously reported in the literature. In this work, we report three types of ^{13}C−^{17}O heteronuclear correlation solid-state NMR experiments under MAS conditions, all of which are based on the Dipolar-mediated Refocused Insensitive Nuclei Enhanced by Polarization Transfer (D-RINEPT) scheme[19−21] with the symmetry-based $SR4_1^2$ recoupling sequence[22] for coherence transfer between ^{13}C and ^{17}O nuclei. The primary goal is to show that overlapping ^{17}O NMR signals can be resolved in the high-resolution ^{13}C dimension via the proposed ^{13}C−^{17}O correlation experiments.
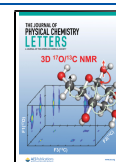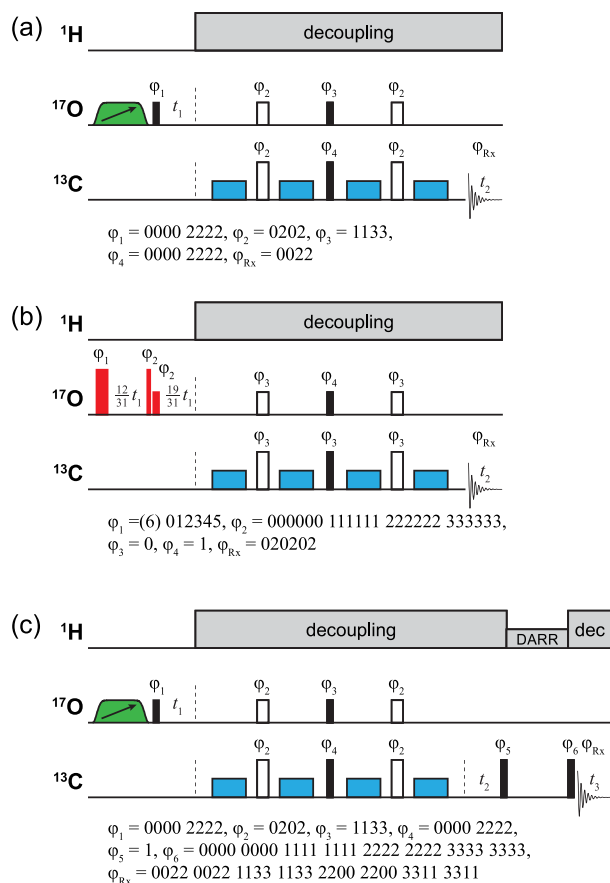
Figure 1 depicts the pulse sequences used in the three ^{17}O $\rightarrow$ ^{13}C correlation experiments. In the first experiment, we start


Figure 1. Pulse sequences and associated phase cycling schemes for the (a) 2D D-RINEPT, (b) 2D MQ-D-RINEPT, and (c) 3D D-RINEPT/DARR OCC experiments. SR4$_1^2$ ^{13}C$-^{17}$O dipolar recoupling blocks are shown in blue, while off-resonance WURST pulses used to enhance ^{17}O CT polarization are shown in green. The filled and open rectangles represent $\pi/2$- and π-pulses, respectively. In (b), the red pulses and interleaved t_1 delays on the ^{17}O channel (before the dashed line) represent a split-t_1 3Q SPAM-MQMAS sequence, which is used to achieve ^{17}O isotropic evolution. All phase cycle values are given as multiples of 90°, except for the φ_1 values in (b) which are given in multiples of 60°. Hypercomplex acquisition is achieved by the method of States et al.[30] on φ_1 for t_1, and additionally on φ_5 for t_2 in (c).

from generation of the ^{17}O single-quantum coherence for the central-transition (CT) enhanced by saturation/inversion of the satellite-transitions with a Wideband Uniform-Rate Smooth Truncation (WURST) sequence.[23−25] After the t_1 evolution period, the ^{17}O coherence is then transferred to ^{13}C by the D-RINEPT scheme where the symmetry-based SR4$_1^2$ recoupling sequence is employed. During the acquisition period t_2, high-power ^{1}H decoupling is applied. The second experiment combines the multiple-quantum MAS (MQMAS) scheme[26,27] with D-RINEPT, which was first introduced by Martineau et al.[28] and termed as the MQ-D-RINEPT experiment. Such an experiment averages the anisotropic second-order quadrupolar broadening to the ^{17}O dimension. The third pulse sequence shown in Figure 1(c) is a new 3D ^{17}O $\rightarrow$ ^{13}C $\rightarrow$ ^{13}C correlation experiment where we combine

^{17}O $\rightarrow$ ^{13}C heteronuclear correlation with ^{13}C $\rightarrow$ ^{13}C homonuclear correlation. The ^{17}O $\rightarrow$ ^{13}C correlation part between t_1 and t_2 is identical to that used in the first two experiments whereas the ^{13}C $\rightarrow$ ^{13}C correlation portion between t_2 and t_3 is achieved with the Dipolar-Assisted Rotational Resonance (DARR) sequence.[29] We will refer to this new 3D ^{17}O $\rightarrow$ ^{13}C $\rightarrow$ ^{13}C correlation experiment as the 3D D-RINEPT/DARR OCC experiment. The main objective of this 3D experiment is to utilize the high spectral resolution in the ^{13}C dimensions (in both ^{13}C diagonal peaks and ^{13}C$-^{13}$C cross peaks) to further separate overlapping ^{17}O NMR signals.

Figure 2 shows the 2D ^{17}O $\rightarrow$ ^{13}C correlation NMR spectra of [1-^{13}C,^{17}O]-Gly/Gly·HCl cocrystal (^{13}C, 98%; ^{17}O, 40%) and [U-^{13}C, 1-^{17}O]-α/β-D-glucose (^{13}C, 98%; ^{17}O, 70%) obtained with the pulse sequence shown in Figure 1(a), together with the corresponding 1D ^{17}O MAS spectra. In the [1-^{13}C,^{17}O]-Gly/Gly·HCl cocrystal, the carboxyl group of the glycine molecule is [^{13}C,^{17}O]-doubly labeled. In this cocrystal compound, there are two types of carboxyl groups in the crystal lattice: C(=O)−OH and COO$^-$. Furthermore, the two O atoms in the carboxylate group, COO$^-$, are crystallographically nonequivalent.[31] As a result, a total of four ^{17}O NMR signals are expected for the [1-^{13}C,^{17}O]-Gly/Gly·HCl cocrystal. As seen from Figure 2(a), the C=O and C−OH signals are well separated in the 1D ^{17}O MAS spectrum while the two signals from the COO$^-$ group overlap. In the 2D ^{17}O $\rightarrow$ ^{13}C correlation spectrum shown in Figure 2(b), the four ^{17}O NMR signals are separated into two groups according to the C atoms that they are attached to. An analysis of F$_1$-slice spectra yielded the following ^{17}O NMR parameters: O1, δ_{iso} = 340 ppm, C_Q = 8.5 MHz, η_Q = 0.0; O2, δ_{iso} = 276 ppm, C_Q = 6.8 MHz, η_Q = 0.55; O3, δ_{iso} = 269 ppm, C_Q = 7.0 MHz, η_Q = 0.60; O4, δ_{iso} = 180 ppm, C_Q = 6.9 MHz, η_Q = 0.0. For this particular compound, the 2D ^{13}C$-^{17}$O correlation experiment does not seem to have any advantage in resolving overlapping ^{17}O NMR signals, because the two overlapping ^{17}O NMR signals happen to attach to the same C atom. However, the high-quality 2D data (obtained with an experimental time of approximately 70 min) demonstrates the feasibility of this proof-of-concept experiment. It is also interesting to note that the F$_1$-slice spectra do not exhibit any distortion in the second-order quadrupole line shapes. In the [U-^{13}C, 1-^{17}O]-α/β-D-glucose sample prepared for this study, the two anomers, α and β, coexist in a ratio of approximately $\alpha:\beta$ = 4:5. As seen from Figure 2(c), the two ^{17}O NMR signals from O1 atoms of the α- and β-anomers severely overlap in the 1D ^{17}O MAS spectrum, making it difficult to extract any useful ^{17}O NMR parameters. In the 2D ^{13}C$-^{17}$O correlation spectrum, shown in Figure 2(d), the two ^{17}O NMR signals become separated in the ^{13}C dimension because the two ^{13}C NMR signals, C1α and C1β, are very well resolved at 94.3 and 90.6 ppm (the line width of the ^{13}C peaks is less than 0.5 ppm). Fitting the F$_1$-slice spectra allowed us to obtain the following ^{17}O NMR parameters: O1α, δ_{iso} = 35 ppm, C_Q = 8.5 MHz, η_Q = 0.95; O1β, δ_{iso} = 42 ppm, C_Q = 8.9 MHz, η_Q = 0.75. It is interesting to note that the isotropic ^{17}O chemical shift difference between O1α and O1β is twice of that between C1α and C1β, demonstrating the sensitivity of ^{17}O NMR to molecular structure and chemical bonding.[3,4,6]

In the ^{17}O $\rightarrow$ ^{13}C correlation spectra in Figure 2, the ^{17}O NMR signals suffer from second-order quadrupole broadening
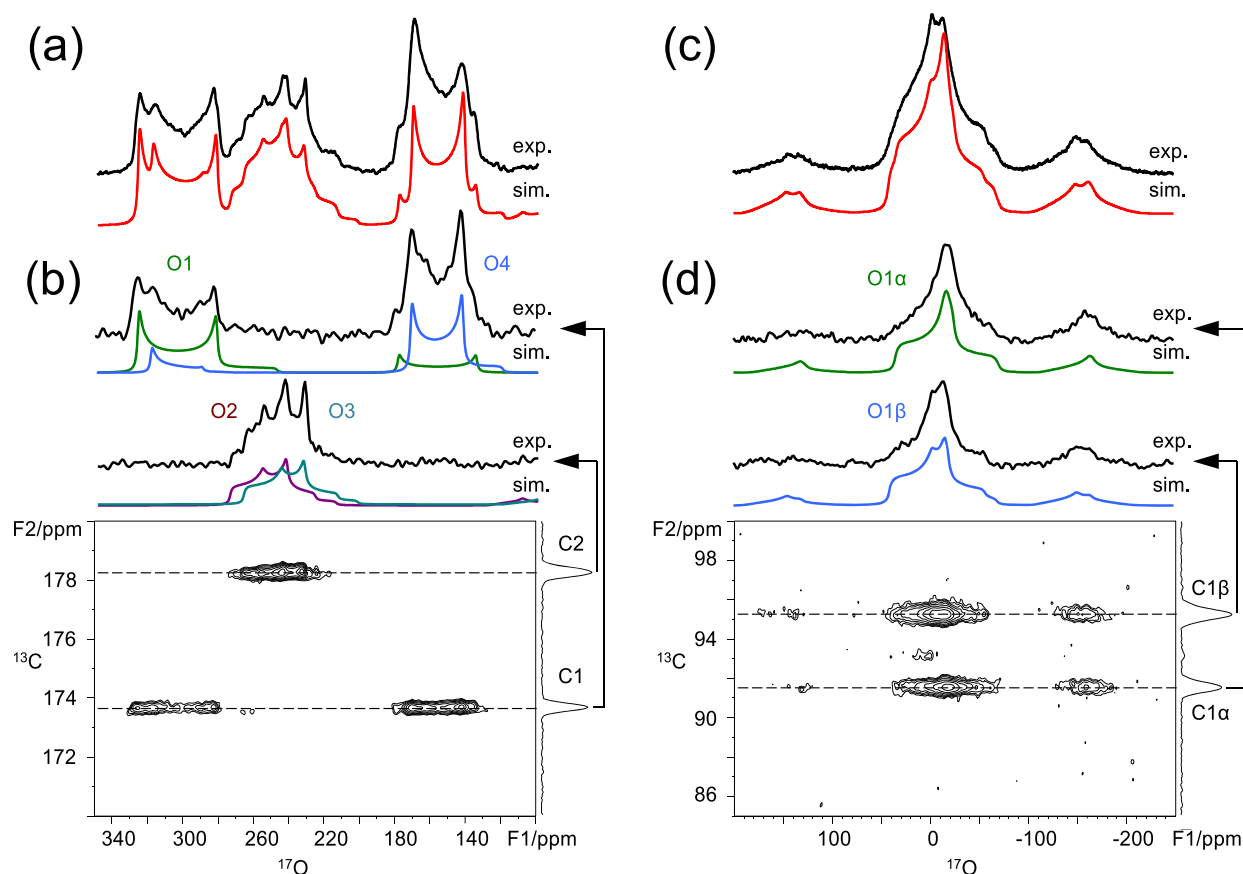
Figure 2. (a) Experimental (black trace) and simulated (red trace) 1D ^{17}O MAS and (b) 2D $^{13}C-^{17}O$ heteronuclear correlation NMR spectra obtained for the $[1-^{13}C,^{17}O]$-Gly/Gly·HCl cocrystal. In (b), a total of 64 complex t_1 increments were collected with 32 transients per increment and a recycle delay of 1.0 s (the total experimental time was 1.2 h). (c) Experimental (black trace) and simulated (red trace) 1D ^{17}O MAS and (d) 2D $^{13}C-^{17}O$ heteronuclear correlation NMR spectra obtained for $[U-^{13}C; 1-^{17}O]$-α/β-D-glucose. In (d), a total of 64 complex t_1 increments were collected with 128 transients per increment and a recycle delay of 0.85 s (the total experimental time was 4.1 h). All spectra were recorded at 18.8 T at a MAS frequency of 16 kHz, with 83 kHz SPINAL-64 ^1H decoupling, and 32 kHz SR4$_1^2$ recoupling.

under MAS conditions. Figure 3 displays the 2D $^{17}O \rightarrow ^{13}C$ MQ-D-RINEPT correlation spectrum obtained for $[U-^{13}C, 1-^{17}O]$-α/β-D-glucose. In this case, the projection of the indirect ^{17}O dimension shows two partially overlapped isotropic peaks for O1α and O1β. However, because the separation between the two ^{13}C NMR signals, C1α and C1β, is greater than 3 ppm with a line width of only 0.5 ppm, the two ^{17}O NMR signals in the 2D $^{13}C-^{17}O$ correlation spectrum are completely resolved. This combined resolving power utilizing the ^{13}C resolution is a significant advantage of the MQ-D-RINEPT experiment over the conventional 2D MQMAS experiment.

Figure 4 shows the results of the 3D D-RINEPT/DARR OCC experiment performed on $[U-^{13}C, 1-^{17}O]$-α/β-D-glucose. Figure 4(a) displays one particular F2−F3 plane that shows the 2D $^{13}C-^{13}C$ correlation spectrum. Since the initial ^{13}C magnetizations were transferred directly from ^{17}O (O1α and O1β) via one-bond dipolar couplings, this particular 2D plane corresponds to a band selective correlation spectrum where only C1α/C1β diagonal signals and their cross peaks to other ^{13}C signals are present. A DARR mixing time of 100 ms was used to ensure that cross peaks from C1 to all other five C atoms in the entire glucose molecule could be observed for each anomer; intermolecular cross peaks between the two anomers were not observed. The ^{13}C signal assignments shown

in Figure 4(a) for α-D-glucose and β-D-glucose are known from previous solid-state ^{13}C NMR studies.[32,33] Figure 4(b) displays four F1−F3 slices to illustrate the advantage of the 3D D-RINEPT/DARR OCC experiment in resolving different ^{17}O NMR signals. The F1−F3 slices for the C1β and C1α diagonal peaks show the separation of the two ^{17}O NMR signals via the two ^{13}C signals with a chemical shift difference of 3.5 ppm. As expected, this is identical to the result of the 2D $^{17}O \rightarrow ^{13}C$ correlation experiment shown in Figure 2(d). In contrast, the two C1β-C2β and C1α-C2α cross peaks exhibit an even larger ^{13}C chemical shift difference, 5.0 ppm, in the F3 dimension. The spread of chemical shift resolution in two dimensions leads to significantly enhanced resolving power as illustrated by the two ^{17}O NMR signals. Similarly, the two ^{17}O NMR signals can also be separated by other "mixed" cross peaks such as C1β-C4β and C1α-C6α. Figure 4(c) shows that, while the diagonal peaks (C1β and C1α) are stronger than the cross peaks (C2β and C2α), they display the same 1D ^{17}O NMR second-order quadrupole line shapes. One can envision that this new 3D OCC strategy can be applied to proteins containing selectively $[U-^{13}C; 1-^{17}O]$-labeled amino acid residues. Thus, the backbone ^{17}O NMR signals can be correlated to both CO and Cα atoms. In principle, similar 3D experiments such as $^{17}O-^{13}C-^{15}N$ can be designed to
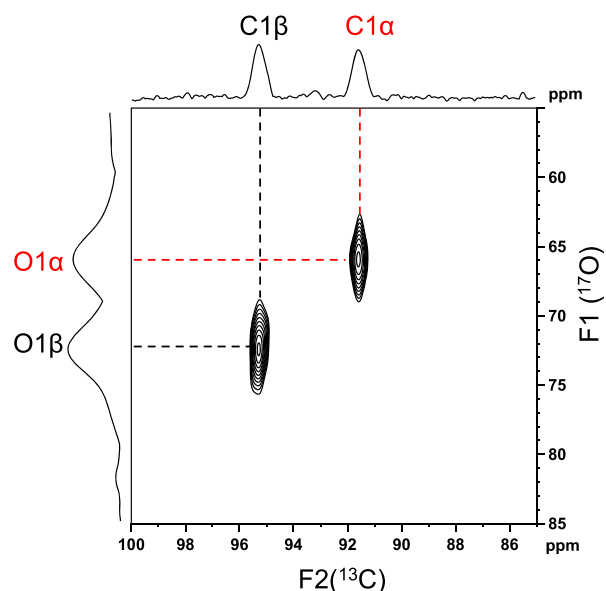
Figure 3. 2D $^{17}O \rightarrow {}^{13}C$ MQ-D-RINEPT spectrum obtained for $[U^{-13}C; 1^{-17}O]$-α/β-D-glucose. A total of 30 complex t_1 increments were collected with 744 transients per increment and a recycle delay of 0.85 s (the total experimental time was 11.2 h). The spectrum was acquired at 18.8 T at a MAS frequency of 16 kHz, with 83 kHz SPINAL-64 ^{1}H decoupling, and 32 kHz SR4$_1^2$ recoupling.

further extend heteronuclear correlations to ^{15}N, thus requiring 4-channel ($^{1}H/{}^{13}C/{}^{17}O/{}^{15}N/$) MAS probes.

All three experiments shown in Figure 1 start from ^{17}O polarization and utilize ^{13}C detection after coherence transfer and time evolution for the indirect dimensions. Such routes have several advantages. First, detecting the nucleus with a higher gyromagnetic ratio gives better receptivity. Second, ^{17}O tends to have shorter T_1 values due to quadrupolar relaxation, allowing more rapid scan repetition. Third, only the ^{13}C signals originating from ^{17}O polarization transferred via D-RINEPT are detected at the end. Other correlation methods such as Dipolar-mediated Heteronuclear Multiple-Quantum Coherence (D-HMQC) require phase cycling to cancel uncorrelated signals, and are therefore more prone to t_1-noise problems.[34] In principle, cross-polarization from ^{1}H can enhance the signals and is used routinely for spin-1/2 nuclei like ^{13}C and ^{15}N. However, for half-integer quadrupolar nuclei, spin-locking under MAS tends to be inefficient and thus cross-polarization results in significantly lower transfer efficiencies than for spin-1/2 nuclei.[35] In this study, we found that starting from ^{17}O polarization enhanced by irradiation of the ^{17}O satellite transitions generally gives higher experimental efficiency and less t_1-noise. The optimal experimental route would likely change if dynamic nuclear polarization (DNP) is applied. DNP is capable of enhancing NMR signals by orders of magnitude providing much needed sensitivity for applications of multidimensional NMR experiments to study quadrupolar nuclei in biological macromolecules. However, the DNP enhancement is generally faster and higher for protons than for more dilute and/or low-γ nuclei. Hence, the experiments presented herein may need to be reimagined when combined with DNP so they start from ^{1}H polarization. It is also worth mentioning that in Figure 1 multiple-pulse dipolar recoupling is applied to the ^{13}C nuclei. For quadrupolar nuclei under MAS, applying strong radio frequency pulses can lead to leakage of central-transition
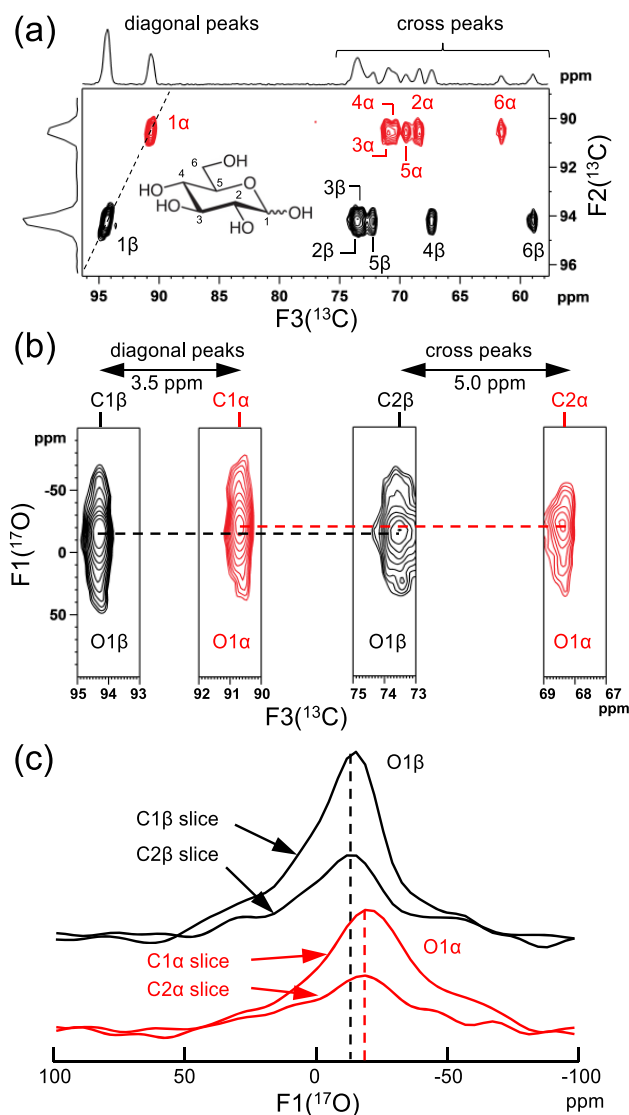
Figure 4. Results from the 3D D-RINEPT/DARR OCC spectrum obtained for $[U^{-13}C; 1^{-17}O]$-α/β-D-glucose. (a) A F2−F3 plane at F1(^{17}O) = −20.8 ppm showing 2D $^{13}C-{}^{13}C$ homonuclear correlation. (b) Four F1−F3 2D slice spectra showing C1β (F2 = 94.1 ppm) and C1α (F2 = 90.6 ppm) diagonal peaks and C1β-C2β (F2 = 94.1 ppm) and C1α−C2α (F2 = 90.6 ppm) cross peaks. (c) The 1D ^{17}O F1-slice spectra from the diagonal (C1β and C1α) cross peaks (C2β and C2α) showing the same line shape for each oxygen site. The 3D spectrum was acquired at 18.8 T under the following conditions: MAS frequency of 16 kHz, 83 kHz SPINAL-64 ^{1}H decoupling, 32 kHz SR4$_1^2$ recoupling, and a cw DARR mixing time of 100 ms with a ^{1}H rf field matching the sample spinning frequency of 16 kHz. The number of complex t_1 and t_2 increments were 24 and 12, respectively. A total of 224 transients were collected per increment with a recycle delay of 0.85 s (total experimental time was 69.1 h).

coherence to other transitions. Avoiding such signal loss by restricting recoupling pulses to the ^{13}C nuclei may be one of the reasons that one-step D-RINEPT transfer used in this study appears to be more efficient than the previously reported $^{13}C \rightarrow {}^{17}O \rightarrow {}^{13}C$ ZF-TEDOR sequence,[13] which applied recoupling π-pulses to the ^{17}O channel.

In summary, we have demonstrated three $^{17}O \rightarrow {}^{13}C$ correlation experiments for studying organic/biological solids

under MAS conditions. These experiments exhibit greatly improved sensitivity over previous reports of ^{13}C−^{17}O correlation solid-state NMR spectroscopy. The new 3D D-RINEPT/DARR OCC experiment provides significant resolving power to separate overlapping ^{17}O NMR signals. The success of the three ^{13}C−^{17}O correlation experiments reported in this study paves the way for ^{17}O solid-state NMR studies of proteins. It is likely that incorporation of DNP into these ^{13}C−^{17}O heteronuclear correlation experiments will further enhance the power of ^{17}O solid-state NMR spectroscopy using oxygen chemical shift and quadrupole coupling as sensitive probes for complex molecules like proteins. Research in this direction is underway in our laboratories.

■ AUTHOR INFORMATION

Corresponding Author

Gang Wu − *Department of Chemistry, Queen's University, Kingston, Ontario K7L 3N6, Canada;* ● orcid.org/0000-0002-0936-9432; Email: wugang@queensu.ca

Authors

Ivan Hung − *Center for Interdisciplinary Magnetic Resonance, National High Magnetic Field Laboratory, Tallahassee, Florida 32310, United States;* ● orcid.org/0000-0001-8916-739X

Zhehong Gan − *Center for Interdisciplinary Magnetic Resonance, National High Magnetic Field Laboratory, Tallahassee, Florida 32310, United States;* ● orcid.org/0000-0002-9855-5113

Complete contact information is available at:
https://pubs.acs.org/10.1021/acs.jpclett.1c02465

Notes

The authors declare no competing financial interest.

■ REFERENCES

(1) Lemaitre, V.; Smith, M. E.; Watts, A. A review of oxygen-17 solid-state NMR of organic materials - towards biological applications. *Solid State Nucl. Magn. Reson.* **2004**, *26*, 215−235.

(2) Wu, G. Solid-state ^{17}O NMR studies of organic and biological molecules. *Prog. Nucl. Magn. Reson. Spectrosc.* **2008**, *52*, 118−169.

(3) Wu, G. Solid-State ^{17}O NMR studies of organic and biological molecules: Recent advances and future directions. *Solid State Nucl. Magn. Reson.* **2016**, *73*, 1−14.

(4) Wu, G. ^{17}O NMR studies of organic and biological molecules in aqueous solution and in the solid state. *Prog. Nucl. Magn. Reson. Spectrosc.* **2019**, *114−115*, 135−19.

(5) Paulino, J.; Yi, M.; Hung, I.; Gan, Z.; Wang, X.; Chekmenev, E. Y.; Zhou, H.-X.; Cross, T. A. Functional statbility of water wire-carbonyl interactions in an ion channel. *Proc. Natl. Acad. Sci. U. S. A.* **2020**, *117*, 11908−11915.

(6) Palmer, J.; Wu, G. Recent developments in ^{17}O NMR studies of organic and biological molecules in the solid state. *Annu. Rep. NMR Spectrosc.* **2021**, *103*, 1−46.

(7) Lin, B.; Hung, I.; Gan, Z.; Chien, P.-H.; Spencer, H. L.; Smith, S. P.; Wu, G. ^{17}O NMR studies of yeast ubiquitin in aqueous solution and in the solid state. *ChemBioChem* **2021**, *22*, 826−829.

(8) Amoureux, J.-P.; Trébosc, J.; Delevoye, L.; Lafon, O.; Hu, B.; Wang, Q. Correlation NMR spectroscopy involving quadrupolar nuclei. *Solid State Nucl. Magn. Reson.* **2009**, *35*, 12−18.

(9) Deschamps, M.; Massiot, D. Correlation experiments involving half-integer quadrupolar nuclei. In *NMR of Quadrupolar Nuclei in Solid Materials*; Wasylishen, R. E., Ashbrook, S. E., Wimperis, S., Eds.; John Wiley & Sons Ltd.: Chichester, U.K., 2012; pp 178−198.

(10) Tricot, G.; Trébosc, J.; Pourpoint, F.; Gauvin, R.; Delevoye, L. The D-HMQC MAS-NMR technique: An efficient tool for the editing of through-space correlation spectra between quadrupolar and spin-1/2 (^{31}P, ^{29}Si, ^{1}H, ^{13}C) nuclei. *Annu. Rep. NMR Spectrosc.* **2014**, *81*, 145−184.

(11) Nagashima, H.; Lilly Thankamony, A. S.; Trébosc, J.; Montagne, L.; Kerven, G.; Amoureux, J.-P.; Lafon, O. Observation of proximities between spin-1/2 and quadrupolar nuclei in solids: Improved robustness to chemical shielding using adiabatic symmetry-based recoupling. *Solid State Nucl. Magn. Reson.* **2018**, *94*, 7−19.

(12) Carnahan, S. L.; Lampkin, B. J.; Naik, P.; Hanrahan, M. P.; Slowing, I. I.; VanVeller, B.; Wu, G.; Rossini, A. J. Probing O−H bonding through proton detected ^{1}H−^{17}O double resonance solid-state NMR spectroscopy. *J. Am. Chem. Soc.* **2019**, *141*, 441−450.

(13) Keeler, E. G.; Michaelis, V. K.; Colvin, M. T.; Hung, I.; Gor'kov, P. L.; Cross, T. A.; Gan, Z.; Griffin, R. G. ^{17}O MAS NMR correlation spectroscopy at high magnetic fields. *J. Am. Chem. Soc.* **2017**, *139*, 17953−17963.

(14) Chopin, L.; Vega, S.; Gullion, T. A MAS NMR method for measuring ^{13}C-^{17}O distances. *J. Am. Chem. Soc.* **1998**, *120*, 4406−4409.

(15) Goldbourt, A.; Vega, S.; Gullion, T.; Vega, A. J. Interatomic distance measurement in solid-state NMR between a spin-1/2 and a spin-5/2 using a universal REAPDOR curve. *J. Am. Chem. Soc.* **2003**, *125*, 11194−11195.

(16) Chen, L.; Lu, X.; Wang, Q.; Lafon, O.; Trébosc, J.; Deng, F.; Amoureux, J.-P. Distance measurement between a spin-1/2 and a half-integer quadrupolar nuclei by solid-state NMR using exact analytical expressions. *J. Magn. Reson.* **2010**, *206*, 269−273.

(17) Hung, I.; Uldry, A.-C.; Becker-Baldus, J.; Webber, A. L.; Wong, A.; Smith, M. E.; Joyce, S. A.; Yates, J. R.; Pickard, C. J.; Dupree, R.; Brown, S. P. Probing heteronuclear ^{15}N-^{17}O and ^{13}C-^{17}O connectivities and proximities by solid-state NMR spectroscopy. *J. Am. Chem. Soc.* **2009**, *131*, 1820−1834.

(18) Rees, G. J.; Day, S. P.; Barnsley, K. E.; Iuga, D.; Yates, J. R.; Wallis, J. D.; Hanna, J. V. Measuring multiple ^{17}O-^{13}C J-couplings in naphthalaldehydeic acid: a combined solid state NMR and density functional theory approach. *Phys. Chem. Chem. Phys.* **2020**, *22*, 3400−3413.

(19) Fyfe, C. A.; Mueller, K. T.; Grondey, H.; Wong-Moon, K. C. Dipolar dephasing between quadrupolar and spin-12 nuclei. REDOR and TEDOR NMR experiments on VPI-5. *Chem. Phys. Lett.* **1992**, *199*, 198−204.

(20) Sørensen, O. W.; Ernst, R. R. Elimination of spectral distortion in polarization transfer experiments. Improvements and comparison of techniques. *J. Magn. Reson.* **1983**, *51*, 477−489.

(21) Trebosc, J.; Hu, B.; Amoureux, J.-P.; Gan, Z. Through-space R^3-HETCOR experiments between spin-1/2 and half-integer quadrupolar nuclei in solid-state NMR. *J. Magn. Reson.* **2007**, *186*, 220−227.

(22) Brinkmann, A.; Kentgens, A. P. M. Proton-selective ^{17}O-^{1}H distance measurements in fast magic-angle-spinning solid-state NMR spectroscopy for the determination of hydrogen bond lengths. *J. Am. Chem. Soc.* **2006**, *128*, 14758−14759.

(23) Kupce, E.; Freeman, R. Adiabatic pulses for wideband inversion and broadband decoupling. *J. Magn. Reson., Ser. A* **1995**, *115*, 273−276.

(24) Kupce, E.; Freeman, R. Optimized adiabatic pulses for wideband spin inversion. *J. Magn. Reson., Ser. A* **1996**, *118*, 299−303.

(25) Dey, K. K.; Prasad, S.; Ash, J. T.; Deschamps, M.; Grandinetti, P. J. Spectral editing in solid-state MAS NMR of quadrupolar nuclei using selective satellite inversion. *J. Magn. Reson.* **2007**, *185*, 326−330.

(26) Frydman, L.; Harwood, J. S. Isotropic spectra of half-integer quadrupolar spins from bidimensional magic-angle-spinning NMR. *J. Am. Chem. Soc.* **1995**, *117*, 5367−5368.

(27) Medek, A.; Harwood, J. S.; Frydman, L. Multiple-quantum magic-angle spinning NMR: A new method for the study of quadrupolar nuclei in solids. *J. Am. Chem. Soc.* **1995**, *117*, 12779−12787.

(28) Martineau, C.; Bouchevreau, B.; Taulelle, F.; Trébosc, J.; Lafon, O.; Amoureux, J.-P. High-resolution through-space correlations between spin-1/2 and half-integer quadrupolar nuclei using the MQ-D-R-INEPT NMR experiment. *Phys. Chem. Chem. Phys.* **2012**, *14*, 7112−7119.

(29) Takegoshi, K.; Nakamura, S.; Terao, T. $^{13}C-^{1}H$ dipolar-assisted rotational resonance in magic-angle spinning NMR. *Chem. Phys. Lett.* **2001**, *344*, 631−637.

(30) States, D. J.; Haberkorn, R. A.; Ruben, D. J. A two-dimensional nuclear overhauser experiment with pure absorption phase in four quadrants. *J. Magn. Reson.* **1982**, *48*, 286−292.

(31) Natarajan, S.; Muthukrisshnan, C.; Asath Bahadur, S.; Rajaram, R. K.; Rajan, S. S. Reinvestigation of the crystal structure of diglycine hydrochloride. *Z. Kristallogr. - Cryst. Mater.* **1992**, *198*, 265−270.

(32) Pfeffer, P. E.; Hicks, K. B.; Frey, M. H.; Opella, S. J.; Earl, W. L. Complete solid state ^{13}C NMR chemical shift assignments for α-D-glucose, α-D-glucose·H_2O and β-D-glucose. *J. Carbohydr. Chem.* **1984**, *3*, 197−217.

(33) Rossini, A. J.; Zagdoun, A.; Hegner, F.; Schwarzwälder, M.; Gajan, D.; Copéret, C.; Lesage, A.; Emsley, L. Dynamic nuclear polarization NMR spectroscopy of microcrystalline solids. *J. Am. Chem. Soc.* **2012**, *134*, 16899−16908.

(34) Venkatesh, A.; Luan, X.; Perras, F. A.; Hung, I.; Huang, W.; Rossini, A. J. T_1-noise eliminated dipolar heteronuclear multiple-quantum coherence solid-state NMR spectroscopy. *Phys. Chem. Chem. Phys.* **2020**, *22*, 20815−20828.

(35) Vega, A. J. MAS NMR spin locking of half-integer quadrupolar nuclei. *J. Magn. Reson.* **1992**, *96*, 50−68.